Inorganica Chimica Acta 380 (2012) 223–229

Contents lists available at SciVerse ScienceDirect

Inorganica Chimica Acta

journal homepage: www.elsevier.com/locate/ica

# Binding ability of aminophosphonates containing imidazole and pyridine as additional donor systems

Monika Pyrkosz [a], Waldemar Goldeman [b], Elzbieta Gumienna-Kontecka [a,*]

[a] Faculty of Chemistry, University of Wroclaw, F. Joliot-Curie 14, 50-383 Wroclaw, Poland
[b] Department of Organic Chemistry, Faculty of Chemistry, Wroclaw University of Technology, Wybrzeze Wyspianskiego 27, 50-370 Wroclaw, Poland

ARTICLE INFO

*Article history:*
Available online 24 September 2011

Young Investigator Award Special Issue

*Keywords:*
Aminomethylphosphonate ligands
Imidazole
Pyridine
Cu(II) and Ni(II) ions

ABSTRACT

The paper describes solution studies of Cu(II) and Ni(II) complexes of new N-substituted imidazole-2-yl(amino)methylphosphonates. The presence of the 2-imidazole ring makes studied phosphonates very efficient ligands, with nickel(II) ions chelation much more effective than by the previously designed 4-imidazole analogs. Introduction of *ortho*-pyridine as additional donor in the side chain further increases the binding ability. The effectiveness of this compound is due to chelation of metal ions through imidazol, imino and pyridine nitrogen donors.



## 1. Introduction

Phosphonates have been widely recognized as ligands that are able to form stable complexes with a wide variety of metal ions [1]. Their chelating properties were intensively studied with regard to applications as chelating agents used in analytical chemistry, for the industrial cleaning, removal of toxic metal ions from environment or as corrosion inhibitors, to give only few examples. The beginning of biological career of phosphonates is strongly connected to the discovery in the 1940s of aminophosphonic acids in living organisms [2]. Later on the potential of phosphonates as natural phosphate mimics was recognized [3]. The strong structural relation to natural compounds, together with high stability and low toxicity, caused their possible activity as antimetabolites and competitors for various cellular receptors and molecules. Aminophosphonates, for example, are able to recognize the active centers of enzymes, and by creating appropriate complexes with the metal ions within perform their inhibition [4–6]. Moreover recent papers demonstrate that the chemistry of phosphonates and their complexes show potential power for the design and preparation of nanomaterials [5]. The phosphonic group can be used as the molecular tool in recognition and sensing of biologically relevant molecules, drug delivery and treatment or as a linker between inorganic and organic part of the bio-device.

Stimulated by their applications, and because of the ease of attaching the phosphonic acid group to the organic moiety, the massive number and diversity of ligands were designed, synthesized and studied. Recent works carried in our group on aminophosphonate ligands showed that introduction of additional binding groups, like heterocyclic side chains drastically changes ligands chelating ability [7–10]. We report here an extension of these studies and present binding ability towards Cu(II) and Ni(II) of new aminophosphonates bearing imidazole and pyridine as additional donor groups.

## 2. Experimental

### 2.1. Synthesis of ligands

The N-substituted imidazole-2-yl(amino)methylphosphonic acids (ligands $\mathbf{L}^1$–$\mathbf{L}^5$, Scheme 1) were prepared by the methodology described earlier for the appropriate pyridine [11] and 4(5)-imidazole [12] derivatives. Thus, the ligands were synthesized in reaction of imines (prepared from imidazole-2-carboxaldehyde and amines) and tris(trimethylsilyl) phosphite (generated *in situ* from triethyl or trimethyl phosphite and bromotrimethylsilane) to give the silylated intermediates which after treating with methanol gave the title compounds (Scheme 2) [13].

### 2.2. Physico-chemical measurements

*Starting materials and solvents:* The solution studies were carried out in bidistilled water. All the chemicals were commercial products of reagent grade and were used without further purification. Copper(II) solutions were prepared from $Cu(ClO_4)_2{\cdot}6H_2O$ (Aldrich) and nickel(II) solutions from $Ni(ClO_4)_2{\cdot}6H_2O$ (Aldrich).

* Corresponding author. Fax: +48 71 3757342.
*E-mail address:* elzbieta.gumienna-kontecka@chem.uni.wroc.pl(E. Gumienna-Kontecka).

0020-1693/$ - see front matter © 2011 Elsevier B.V. All rights reserved.
doi:10.1016/j.ica.2011.09.024

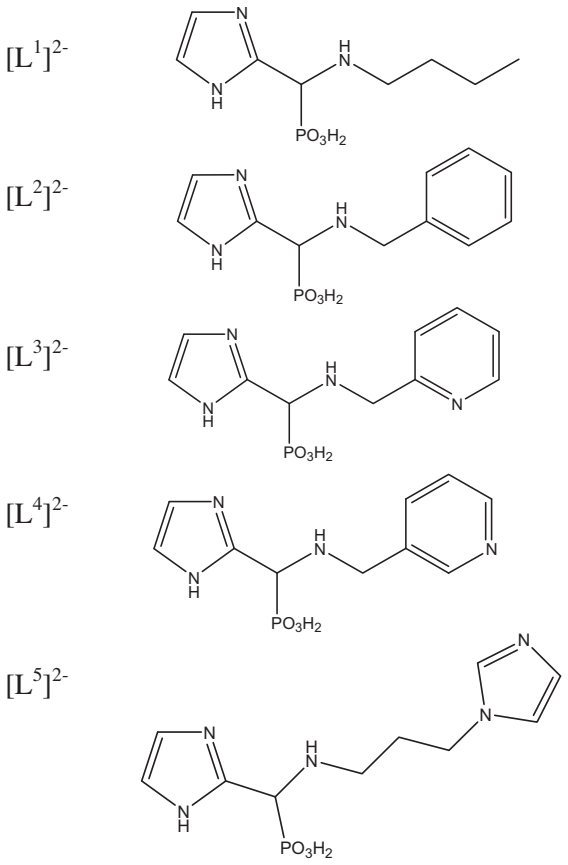


**Scheme 1.** The chemical structures of studied aminophosponates.

The potentiometric titrations were performed using an automatic titrator system Titrando 809 (Metrohm) with a combined glass electrode (Mettler Toledo InLab Semi-Micro) filled with 3 M KCl (Mettler Toledo) in water. The electrode was calibrated daily in hydrogen ion concentration using $HClO_4$ (Applichem) [14]. Carbonate-free NaOH solution (0.1 M Aldrich) was standardized by titration with potassium hydrogen phthalate (Fluka, Puriss, PA). The ionic strength was fixed at $I = 0.1$ M with $NaClO_4$ (Fluka, Puriss, PA). The experiments were carried out at constant temperature of 25 ± 0.2 °C. A stream of argon, pre-saturated with water vapor, was passed over the surface of the solution. The ionic product of water for these conditions was $10^{-13.77}$ mol$^2$ dm$^{-6}$. All the titrations were carried out on a 3 mL samples. Metal–ligand system titrations were performed on solutions of ligand concentrations of 2–4.2 × $10^{-3}$ M and metal-to-ligand molar ratios of 1:1, 1:2, 1:3 and 1:4. The potentiometric data (about 140 points collected over the pH range 2.2–11.0) were refined with the SUPERQUAD [15] program which uses non-linear least-squares methods [16]. Potentiometric data points were weighted by a formula allowing greater pH errors in the region of an end-point than elsewhere. The weighting factor $W_i$ is defined as the reciprocal of the estimated variance of measurements: $W_i = 1/\sigma_i^2 = 1/[\sigma_E^2 + (\delta E/\delta V)^2\sigma V^2]$ where $\sigma_E^2$ and $\sigma_V^2$ are the estimated variances of the potential and volume readings, respectively. The constants were refined by minimizing the error-square sum, $U$, of the potentials. The quality of fit was judged by the values of the sample standard deviation, $S$, and the goodness of fit, $\chi^2$. The scatter of residuals versus pH was reasonably random, without any significant systematic trends, thus indicating a good fit of the experimental data. The successive protonation constants were calculated from the cumulative constants determined with the program. The uncertainties in the log$K$ values correspond to the added standard deviations in the cumulative constants. The distribution curves of the complexes as a function of pH were calculated using the HYSS2006 program [17].

Additionally, a combined potentiometric and $^1$H/$^{31}$P NMR titrations were carried out. $^{31}$P NMR spectra were recorded at 25 °C, at 202.4 and 242.9 MHz, respectively, on a Bruker Avance 500 and Bruker Avance III 600 MHz spectrometers. All measurements were made in $D_2O$, with concentration of ligands of 3 × $10^{-2}$ M and (40%) $H_3PO_4$ used as an external reference for $^{31}$P. Measured pH* was not corrected for the isotopic effect and was adjusted by addition of concentrated NaOD or DCl solutions.

To probe the coordination properties of the new ligands with Cu(II) and Ni(II), a UV–Vis spectrophotometric titrations in the range of d–d bands (400–800 nm) were recorded on a Varian CARY 300 spectrophotometer in a Hellma quartz optical cell (1 cm). Electron paramagnetic resonance spectra were collected on a Bruker ESP 300E spectrometer at X-band frequency (9.4 GHz) at 77 K. EPR spectra were performed in the ethylene glycol–water (1:2 v/v) solution. The metal ions concentrations were 2 × $10^{-3}$ M and metal-to-ligand molar ratio varied from 1:1 to 1:4. The spectroscopic parameters were obtained at the maximum concentration of the particular species as indicated by the potentiometric calculations. For Cu(II)/Ni(II)–**L**$^3$ systems, the combined potentiometric and UV–Vis titrations were recorded using a Varian CARY 50 UV/Vis spectrophotometer fitted with Varian optical fibers (Technologies, Inc. 908.707.1009, Stainless Steel) and immersion probe made of quartz suprazil (Varian, Technologies Inc., 973.984.9092, 10 mm path). The initial pH of 15 mL complex samples was adjusted to be about 2, and the titration of the solution was then carried out by addition of known volumes of $HClO_4$ or NaOH. The acid titration was carried out till the disappearance of the complex band and pH was calculated from acid concentration. The spectrophotometric data were analysed with Specfit [18–21] program which adjust the absorptivities and the stability constants of the species formed at equilibrium. Specfit uses factor analysis to reduce the absorbance

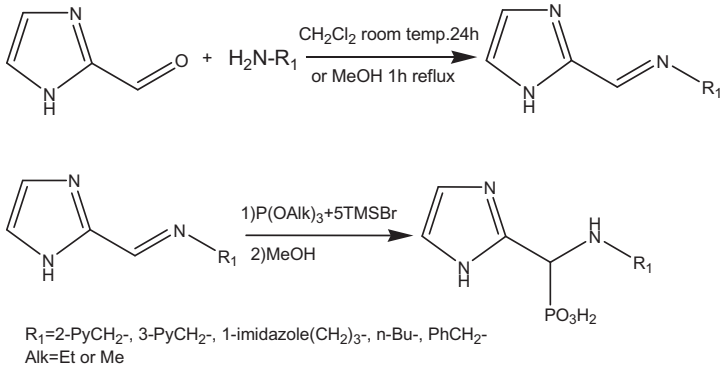


**Scheme 2.** Synthesis of N-substituted imidazole-2-yl-(amino)methylphosphonic acids.

**Table 1**
Protonation ($\log\beta^{H}$) and stability constants ($\log\beta$) of copper(II) and nickel(II) complexes with the N-substituted imidazole-2-yl(amino)methylphosphonates $\mathbf{L}^1$–$\mathbf{L}^5$ in aqueous solution.[a]

| Assignments | Compounds | | | | |
|---|---|---|---|---|---|
| | $\mathbf{L}^1$ | $\mathbf{L}^2$ | $\mathbf{L}^3$ | $\mathbf{L}^4$ | $\mathbf{L}^5$ |
| $\log\beta_1^H$ | 9.21 (9) | 8.82(1) | 8.41(1) | 8.50(1) | 8.70(2) |
| $\log\beta_2^H$ | 14.71 (1) | 14.42(2) | 15.12(2) | 14.17(2) | 15.80(2) |
| $\log\beta_3^H$ | 18.12 (2) | 17.39 (3) | 19.64 (3) | 18.92 (3) | 21.19(3) |
| $\log\beta_4^H$ | – | – | 21.23(4) | 20.90 (5) | 23.95(3) |
| $\log K^{H}$ ($NH_2^+$) | 9.21 | 8.82 | 8.41 | 8.50 | 8.70 |
| $\log K^{H}$ ($NH_{imid}^+$) | 5.50 | 5.60 | 6.71 | 5.67 | 7.10 |
| $\log K^{H}$ ($NH_{imid}^+$) | – | – | – | – | 5.39 |
| $\log K^{H}$ ($NH_{pyr}^+$) | – | – | 4.52 | 4.76 | – |
| $\log K^{H}$ ($PO_3H^-$) | 3.40 | 2.97 | 1.59 | 1.98 | 2.76 |
| $\log\beta$ $[CuH_2L]^{2+}$ | – | – | – | 18.81(5) | 21.56(10) |
| $\log\beta$ $[CuHL]^+$ | 16.86(2) | 16.08(2) | – | – | – |
| $\log\beta$ [CuL] | | | 19.2(5) | | |
| $\log\beta$ $[CuH_4L_2]^{2+}$ | – | – | – | 37.30(7) | 44.93(1) |
| $\log\beta$ $[CuH_3L_2]^+$ | – | – | – | 33.66(6) | 40.78(4) |
| $\log\beta$ $[CuH_2L_2]$ | 32.32 (3) | 31.36 (2) | – | 29.30(6) | 34.64(6) |
| $\log\beta$ $[CuHL_2]^-$ | 26.32(6) | 26.97 (5) | 34.4 (5) | 24.24(7) | 27.88(5) |
| $\log\beta$ $[CuL_2]^{2-}$ | 19.01(8) | 20.41 (9) | 28.2 (5) | 17.87(10) | 20.57(7) |
| $\log\beta$ $[CuL_2(OH)]^{3-}$ | 8.14(12) | 9.90(12) | – | – | – |
| p$K$ $[CuH_4L_2]^{2+}$ | – | – | – | 3.64 | 4.15 |
| p$K$ $[CuH_3L_2]^+$ | – | – | – | 4.36 | 6.14 |
| p$K$ $[CuH_2L_2]$ | 6.00 | 4.39 | – | 5.06 | 6.78 |
| p$K$ $[CuHL_2]^-$ | 7.19 | 6.56 | 6.2 | 6.37 | 7.31 |
| p$K$ $[CuL_2]^{2-}$ | 10.87 | 10.51 | – | – | – |
| $\log\beta$ $[NiH_2L]^{2+}$ | – | – | – | – | 22.03(5) |
| $\log\beta$ $[NiHL]^+$ | 15.64(2) | 15.76(3) | – | – | – |
| $\log\beta$ [NiL] | | | 21.9(4) | | |
| $\log\beta$ $[NiH_4L_2]^{2+}$ | – | – | – | 40.33(3) | 43.78(2) |
| $\log\beta$ $[NiH_3L_2]^+$ | – | – | – | – | 40.54(2) |
| $\log\beta$ $[NiH_2L_2]$ | 30.22(4) | 28.73 (12) | – | 31.95(6) | 34.56(11) |
| $\log\beta$ $[NiHL_2]^-$ | 27.29(3) | 26.06(5) | 39.7(3) | 27.41(5) | 27.94(9) |
| $\log\beta$ $[NiL_2]^{2-}$ | 19.45(6) | 19.74(8) | 35.1(4) | 22.70(6) | 20.90(12) |
| $\log\beta$ $[NiL_2(OH)]^{3-}$ | 10.98(7) | 12.12(10) | – | 15.77(9) | 12.66(16) |
| p$K$ $[NiH_4L_2]^{2+}$ | – | – | – | – | 3.24 |
| p$K$ $[NiH_3L_2]^+$ | – | – | – | – | 5.98 |
| p$K$ $[NiH_2L_2]^-$ | 2.93 | 2.67 | – | 4.54 | 6.62 |
| p$K$ $[NiHL_2]$ | 7.84 | 6.32 | 4.6 | 5.34 | 7.04 |
| p$K$ $[NiL_2]^{2-}$ | 8.47 | 7.62 | – | 6.93 | 8.24 |

[a] $I$ = 0.1 M ($NaClO_4$), $T$ = 25.0(2) °C. The reported errors on $\log\beta$ are given as $1\sigma$.

matrix and to extract the eigen values prior to the multiwavelength fit of the reduced data set according to the Marquardt algorithm [22,23].

## 3. Results and discussion

### 3.1. Protonation constants

To evaluate the coordination properties of the studied ligands (Scheme 1) towards metal ions, first it was necessary to determine their acid-base properties. The fully protonated forms of the ligands possess four $\mathbf{L}^1$–$\mathbf{L}^2$ or five $\mathbf{L}^3$–$\mathbf{L}^5$ dissociable protons, respectively. All studied ligands have one dissociable proton at the imino nitrogen, one at the imidazole moiety and two at the phosphonic function. Additional proton in $\mathbf{L}^3$–$\mathbf{L}^5$ derives from the pyridine or additional imidazole ring. Under our experimental conditions, pH 2–11, we could determine three ($H_3L^+$, $\mathbf{L}^1$–$\mathbf{L}^2$) or four ($H_4\mathbf{L}^{2+}$, $\mathbf{L}^3$–$\mathbf{L}^5$) protonation constants (Table 1).

In order to assign the successive protonation constants to particular protonation sites we have used a combination of potentiometry and NMR spectroscopy, pH*–NMR titrations (pH* means pH not corrected for the isotopic effect). Chosen examples showing the chemical shifts of particular nuclei ($^1$H or $^{31}$P) of ligands $\mathbf{L}^1$, $\mathbf{L}^3$ and $\mathbf{L}^4$ as a function of pH* are shown in Fig. 1. Detailed analysis[1] shows that the shifts of $^{31}$P phosphorus reflect protonation process of almost all groups, especially in $\mathbf{L}^3$ (Fig. 1a–c). The shifts of $^1$H protons of the pyridine moiety in $\mathbf{L}^4$ (Fig. 1f) mirror the protonation of its own nitrogen ($\log K \sim 4.7$) and of the phosphonate function ($\log K \sim 2$). For the analog with the pyridine in ortho- position, $\mathbf{L}^3$, $^1$H shifts of the protons from the pyridine moiety, as well as from the imidazole function, indicate two not well separated $\log K$s: of about 4.5 and 6.5 (Fig. 1e and f). pH* dependent shifts of $^1$H of imidazole of $\mathbf{L}^1$ and $\mathbf{L}^4$ ligands reproduce three steps corresponding to protonation of the imino, imidazole and phosphonate functions (Fig. 1g for $\mathbf{L}^1$ and 1i for $\mathbf{L}^4$). Analysis of the last two spectra in addition to $^{31}$P–pH* profile was especially valuable to confirm the difference between the protonation constant of the phosphonate function ($\log K$ = 3.40 for $\mathbf{L}^1$ versus 1.98 for $\mathbf{L}^4$). Therefore, based on previous examples [10,12,24,25] and taking into account current pH*–NMR study, we can conclude that for all five ligands, the most basic constant corresponds to the protonation of the nitrogen of the secondary amino group (Table 1). Substitution of the butyl group ($\mathbf{L}^1$, $\log K \sim 9.2$) by aromatic ring ($\mathbf{L}^2$), pyridine ($\mathbf{L}^3$ and $\mathbf{L}^4$) or imidazole moiety ($\mathbf{L}^5$) decreases this constant of about 0.4–0.6 log units. This effect comes from an electron-withdrawing effect of the aromatic ring. The second protonation constant, assigned to the imidazole moiety, was increased from $\log K \sim 5.6$ for $\mathbf{L}^1$, $\mathbf{L}^2$, $\mathbf{L}^4$ and $\mathbf{L}^5$ to $\log K$ of 6.71 for $\mathbf{L}^3$ due to possible interactions with the pyridine ring. Further constant, with $\log K \sim 3$–3.4 for $\mathbf{L}^1$ and $\mathbf{L}^2$ corresponds to stepwise protonation of the $PO_3^{2-}$ group. The possibility of the formation of an intramolecular hydrogen bonding between the 2-imidazole nitrogen and

[1] The analysis was based on a complete set of $^1$H/$^{31}$P shifts as a function of pH*, performed for all ligands (data not shown).

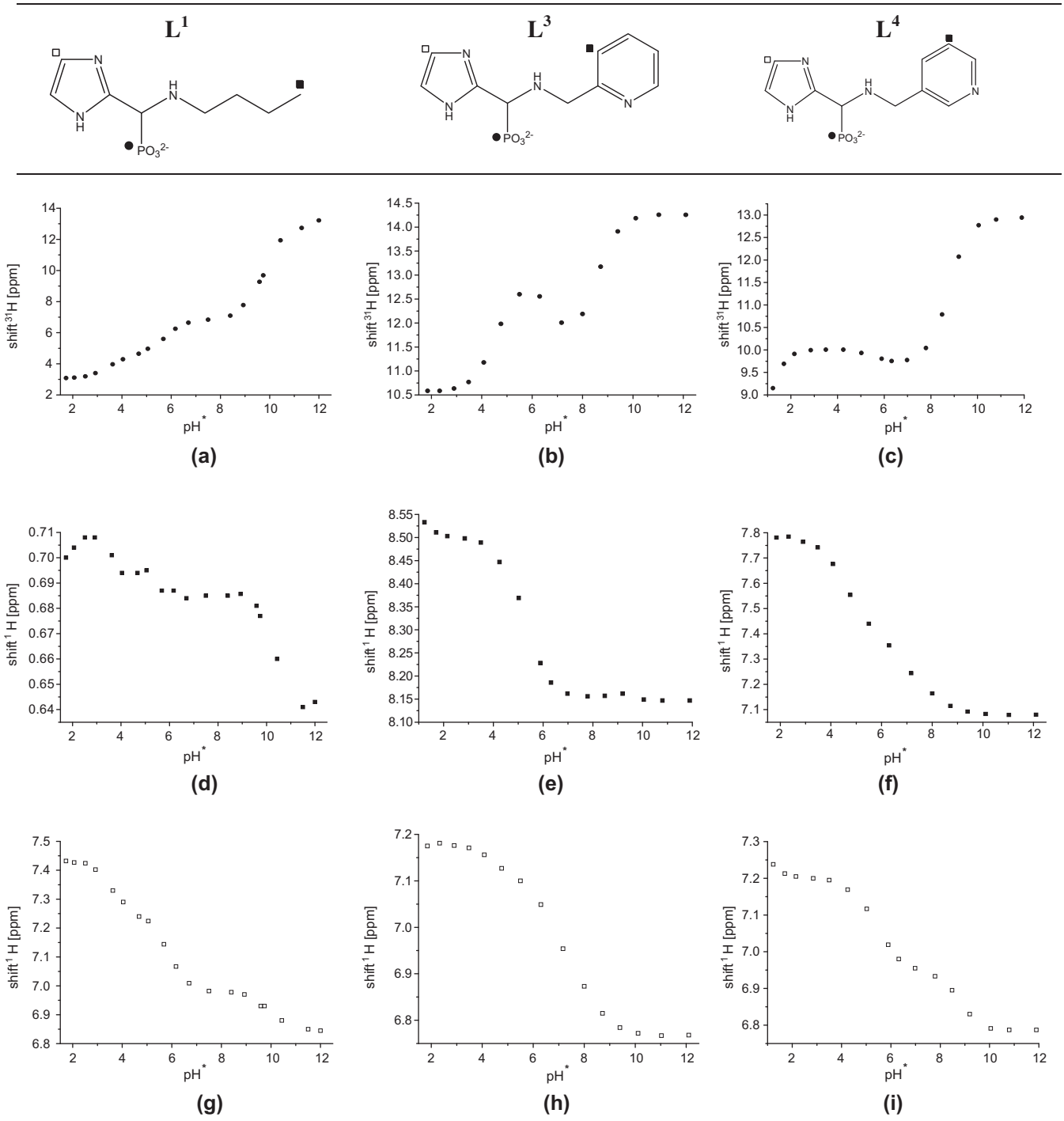


**Fig. 1.** $^{31}P$ and $^{1}H$ NMR titration curves as a function of pH* (pH not corrected for the isotopic effect) performed for $\mathbf{L}^1$, $\mathbf{L}^3$ and $\mathbf{L}^4$ ligands.

phosphonate moiety explains its higher acidity in comparison to simple monophosphonic acids, *e.g.* methylphosphonic acid, with $\log K_{HL} \sim 7.5$ [1]. Its value was further decreased by interactions with pyridine moiety in *ortho*- position ($\log K = 1.59$ for $\mathbf{L}^3$). The protonation of the $PO_3H^-$ group occurs much below pH 2 and constants corresponding to these processes were not determined under our experimental conditions. The value of protonation constant of the pyridine nitrogen was 4.52 for 2-Py analog and 4.76 for 3-Py derivative. Additional imidazole moiety was showing $\log K$ typical for this group ($\log K = 7.1$) [26].

### 3.2. Cu(II) and Ni(II) complexes

All ligands studied in this work have three major binding sites centered at the oxygen atom of phosphonic group, imidazole and amino nitrogen donors. There is also an alternative binding site at the imidazole nitrogen for $\mathbf{L}^5$ and pyridine nitrogen for $\mathbf{L}^3$ and $\mathbf{L}^4$, however it might be competitive only in 2-Py analog $\mathbf{L}^3$. In 3-Py derivative this nitrogen is rather not able to bind to metal ion sitting at the amino-phosphonate binding site of the same ligand molecule, yet it can become a bridging moiety in the dimeric

species [8]. So as to define the solution equilibria between Cu(II) and Ni(II) and the studied ligands and to characterize species formed in solution we have performed potentiometric titrations supported by spectroscopic (UV–Vis and EPR) characterization.

For all ligands, calculations based on potentiometric titrations suggest formation of variously protonated mono- and bis-complexes. Neither dimeric, nor other polynuclear species were detected. The respective stability constants ($\log\beta$) are reported in Table 1 together with the constants corresponding to the successive deprotonation of the complexes. According to the calculations and spectroscopic data, ligands $\mathbf{L}^1$, $\mathbf{L}^2$, $\mathbf{L}^4$ and $\mathbf{L}^5$ form with Cu(II) ions analogous chemical species, with the same coordination pattern. The $\mathbf{L}^1/\mathbf{L}^2$ species differ from $\mathbf{L}^4/\mathbf{L}^5$ ones by proton coming from the pyridine/imidazole rings not participating in metal ion coordination. Therefore to simplify the discussion of the evolution of the species coordination modes' with pH we will present it on an example of Cu(II)–$\mathbf{L}^2$ system. From the species distribution profile shown in Fig. 2 we can see that metal ion complexation starts below pH 2 with the formation of a protonated complex $[CuHL]^+$. The UV–Vis absorption d–d bands centered around 730 nm with $\varepsilon$ of about 25 $M^{-1}cm^{-1}$ (Table 2) indicate that in this species one nitrogen donor besides oxygen atom is bound to the copper ion, $[Cu\{N(imid)O(PO_3^{2-})\}]$. The first monomeric complex is followed by protonated bis-complex $[CuH_2L_2]$, for which the distinct increase of the d–d transitions energy to 685 nm, as well as EPR parameters ($A_{||}$ = 130 and $g_{||}$ = 2.34, Table 2) indicate copper coordination via 2 × $\{N(imid)O(PO_3^{2-})\}$ donor system. The stepwise deprotonation of the $[CuH_2L_2]$ to $[CuHL_2]^-$ and $[CuL_2]^{2-}$ (Table 1) is accompanied by further blue-shift of the d–d bands, as well as increase of $A_{||}$ and decrease of $g_{||}$ (Table 2). These parameters correspond well to three- and four-nitrogens species with $[Cu\{N(imid)N(imino)O(PO_3^{2-})\}\{N(imid)O(PO_3^{2-})\}]$ and $[Cu\{N(imid)N(imino)O(PO_3^{2-})\}_2]$ binding modes for $[CuHL_2]^-$ and $[CuL_2]^{2-}$, respectively. The last species is the major complex predominating over a wide range of pH and its proposed structure is given in Scheme 3. Above pH 9 the hydrolytic $[CuL_2(OH)]^{3-}$ complex starts to be formed, where the deprotonation of equatorially metal-bound water occurs.

The values of stepwise dissociation constants of side chain pyridine and imidazole protons in Cu(II) complexes of $\mathbf{L}^4$ and $\mathbf{L}^5$ (3.64/4.36 and 6.78/7.31, respectively) are very close to dissociation constants of free ligands indicating no involvement of these groups in copper(II) chelation.

Due to the presence of the 2-pyridine in the molecule of ligand $\mathbf{L}^3$, it behaves differently to all other ligands. Preliminary studies showed the formation of first copper(II) complexes already at very acidic solutions (pH ~0.5). Therefore to evaluate their stoichiometry and stability constants we had to use a pH dependent spectroscopic titration based on d–d bands. From the first set of experiments performed in acidic conditions (pH 0.44–2.40, Cu(II)/L = 1, Fig. 3a) we could calculate the stability constant of the [CuL] complex (Table 1). The UV–Vis absorption d–d band centered at around 650 nm with $\varepsilon$ of about 80 $M^{-1}cm^{-1}$ (Table 2, Fig. 4) can indicate that in this species three nitrogen atoms are bound to copper ion, $\{CuN(imid)N(imino)N(pyr)O(PO_3H^-)\}$ (Scheme 4). Also EPR parameters of $A_{||}$ = 175 and $g_{||}$ = 2.12 correspond well to the three nitrogen donors system. Further titration showed a decrease of absorbance intensities with slight blue shift up to pH 5.2 followed by an increase of intensity with concomitant shift to 610 nm at pH 10.5 (Cu(II)/L = 0.5, Fig. 3b). These changes were not observed when the titration was performed for

**Table 2**
Spectroscopic characteristics of Cu(II) and Ni(II) complexes.

| UV–Vis [a] | $\mathbf{L}^1$ | | $\mathbf{L}^2$ | | $\mathbf{L}^3$ | | $\mathbf{L}^4$ | | $\mathbf{L}^5$ | |
|---|---|---|---|---|---|---|---|---|---|---|
| | $\lambda$ | $\varepsilon$ | $\lambda$ | $\varepsilon$ | $\lambda$ | $\varepsilon$ | $\lambda$ | $\varepsilon$ | $\lambda$ | $\varepsilon$ |
| $[CuH_2L]^{2+}$ | – | – | – | – | – | – | 730 | 25 | 730 | 25 |
| $[CuHL]^+$ | 740 | 20 | 730 | 25 | – | – | – | – | – | – |
| [CuL] | – | – | – | – | 650 | 80 | – | – | – | – |
| $[CuH_4L_2]^{2+}$ | – | – | – | – | – | – | 660 | 50 | 680 | 30 |
| $[CuH_3L_2]^+$ | – | – | – | – | – | – | 660 | 50 | 645 | 55 |
| $[CuH_2L_2]$ | 680 | 30 | 685 | 35 | – | – | 660 | 50 | [b] | |
| $[CuHL_2]^-$ | 620 | 65 | 645 | 60 | 640 | 70 | 645 | 60 | 635 | 65 |
| $[CuL_2]^{2-}$ | 585 | 90 | 610 | 85 | 610 | 85 | 620 | 85 | 610 | 85 |
| $[NiH_2L]^{2+}$ | – | – | – | – | – | – | – | – | 650 | 10 |
| $[NiHL]^+$ | 650 | 5 | 660 | 4 | – | – | – | – | – | – |
| $[NiH_4L_2]^{2+}$ | – | – | – | – | – | – | 665 | 3 | 640 | 12 |
| [NiL] | – | – | – | – | 620 | 2 | – | – | – | – |
| $[NiH_3L_2]^+$ | – | – | – | – | – | – | – | – | 630 | 12 |
| $[NiH_2L_2]$ | [b] | [b] | – | – | | | 640 | 4 | 625 | 15 |
| $[NiHL_2]^-$ | 646 | 5 | 655 | 5 | 603 | 3 | 635 | 6 | [b] | |
| $[NiL_2]^{2-}$ | 640 | 8 | 630 | 7 | 581 | 6 | 625 | 9 | 610 | 15 |
| EPR | $A_{II}$ | $g_{II}$ | $A_{II}$ | $g_{II}$ | $A_{II}$ | $g_{II}$ | $A_{II}$ | $g_{II}$ | $A_{II}$ | $g_{II}$ |
| $[CuH_2L]^{2+}$ | – | – | – | – | – | – | 123 | 2.24 | 121 | 2.25 |
| $[CuHL]^+$ | [b] | [b] | – | – | – | – | – | – | | |
| [CuL] | – | – | – | – | 175 | 2.12 | – | – | – | – |
| $[CuH_4L_2]^{2+}$ | – | – | – | – | – | – | 126 | 2.33 | 126 | 2.34 |
| $[CuH_3L_2]^+$ | – | – | – | – | – | – | 126 | 2.33 | 165 | 2.27 |
| $[CuH_2L_2]$ | 132 | 2.33 | 130 | 2.34 | – | – | 126 | 2.33 | 167 | 2.16 |
| $[CuHL_2]^-$ | 167 | 2.27 | 163 | 2.28 | 177 | 2.12 | 165 | 2.28 | 167 | 2.16 |
| $[CuL_2]^{2-}$ | 185 | 2.09 | 177 | 2.10 | 189 | 2.10 | 183 | 2.09 | 180 | 2.09 |

[a] d–d bands. $\lambda$ is given in nm, $\varepsilon$ in $dm^3 mol^{-1} cm^{-1}$, and $A_{II}$ in Gauss. Experimental errors on $\lambda_max$ = ±2 nm and $\varepsilon$ ± 5%.
[b] The spectral parameters were not determined due overlapping of various species.

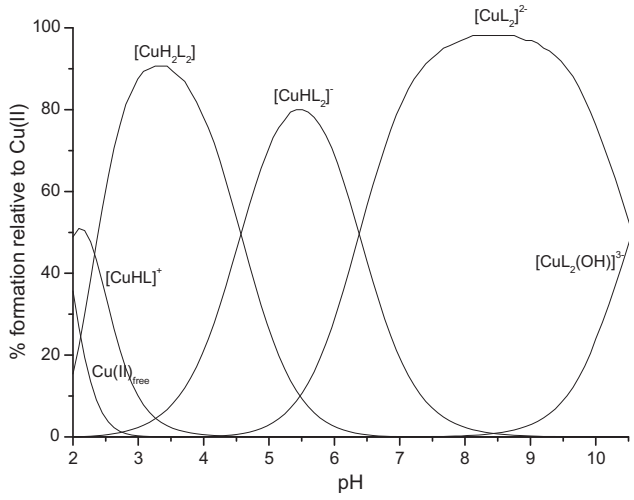


**Fig. 2.** Species distribution diagram for the Cu(II)–$\mathbf{L}^2$ system. [Cu(II)] = 2 × $10^{-3}$ M, metal-to-ligand molar ratio 1:3.

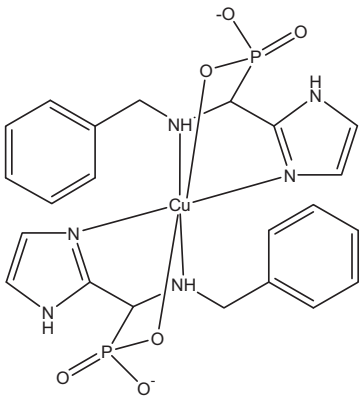


**Scheme 3.** Schematic representation of the proposed structure of the $[CuL_2]^{2-}$ complex of $\mathbf{L}^2$.

metal-to-ligand molar ratio of 1:1. Fixing the value of the [CuL] stability constant and its spectral parameters we could calculate constants for two further complexes: $[CuHL_2]^-$ and $[CuL_2]^{2-}$ (Table 1). The absorption d–d band centered at 640 nm with $\varepsilon$ of 70 $M^{-1}cm^{-1}$ may suggest that in the $[CuHL_2]^-$ complex the binding mode is also realized through three nitrogens, but different ones: $[Cu\{N(imid)N(imino)O(PO_3^{2-})\}\{N(imid)O(PO_3^{2-})\}]$. In the $[CuL_2]^{2-}$ species UV–Vis and EPR parameters confirm participation of four nitrogen atoms in the chelate ring. Although the spectroscopic parameters are similar to the previous four ligands, the participation of the pyridine nitrogen, instead of the phosphonate oxygen, in copper chelation cannot be excluded. The pyridine involvement would explain higher stability of the Cu(II) complexes of $\mathbf{L}^3$ ligand. The species distribution diagram for the Cu(II)–$\mathbf{L}^3$ system is shown in Fig. 5.

Ni(II) ions form with $\mathbf{L}^1$, $\mathbf{L}^2$, $\mathbf{L}^4$ and $\mathbf{L}^5$ ligands mono- and bis-complexes with various protonation degree (Table 1). Again, the $\mathbf{L}^1$/$\mathbf{L}^2$ species differ from $\mathbf{L}^4$/$\mathbf{L}^5$ ones by protons coming from the pyridine/imidazole rings not participating in metal ion coordination. According to the potentiometric calculations, ligands $\mathbf{L}^1$, $\mathbf{L}^2$, $\mathbf{L}^4$ and $\mathbf{L}^5$ form with Ni(II) ions chemical species analogous to Cu(II) complexes. Absorption spectra (Table 2) show that all Ni(II) complexes are of octahedral or pseudo-octahedral geometry. The coordination modes in Ni(II) complexes seem to be the same as in the case of Cu(II) (vide supra). Taking ligand $\mathbf{L}^2$ as an example we can see that the stepwise p$K$ value of the $[NiH_2L_2] \rightarrow [NiHL_2]^- + H^+$ reaction is of 2.7 in comparison to 4.39 for copper(II) (Table 1). Further deprotonation leading to $[NiHL_2]^-$ species is equal to 6.32 for Ni(II) versus 6.56 for Cu(II). These two steps correspond to the deprotonation of the imino moiety from two bound ligands. For all ligands the hydrolysis of Ni(II) complex occurs at lower pH (pH above 6) than for Cu(II) complex (pH above 9). The species distribution diagram for this system is shown in Fig. 6 together with the plot of Ni(II) complexes of its 4-imidazole analog $\mathbf{L}^3$ (imidazole-4-methyl(N-benzylamino)phosphonic acid) and is presented in this way for purpose of other comparison [12]]. Analysis of these speciations shows that the corresponding Ni(II)–$\mathbf{L}^2$ complexes appear at lower pH indicating stronger binding ability of this compound.

pH dependent UV–Vis spectroscopic titration based on d-d bands carried out for Ni(II)–$\mathbf{L}^3$ allow to evaluate stability constants for three complexes: [NiL] $\log\beta = 21.9(4)$, $[NiHL_2]^-$ $\log\beta = 39.7(3)$ and $[NiL_2]^{2-}$ $\log\beta = 35.1(4)$. Spectroscopic parameters corresponding to these species (Table 2) point toward the metal ion binding through three and four nitrogen atoms, like it was in copper(II) complexes (vide supra).

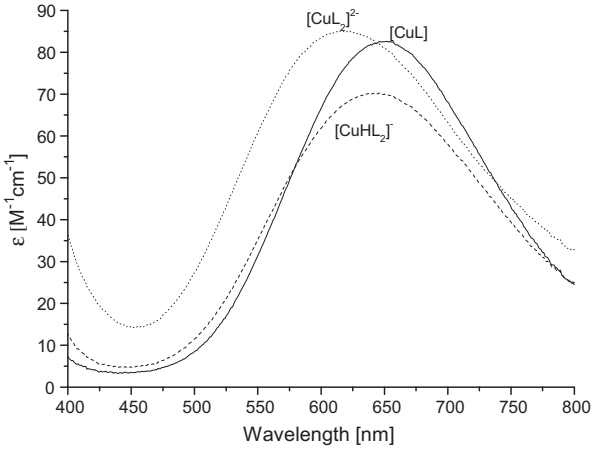


**Fig. 4.** Electronic spectra of the species calculated for Cu(II)–$\mathbf{L}^3$ system.

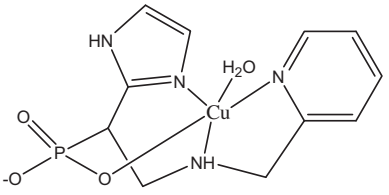


**Scheme 4.** Schematic representation of the proposed structure of the [CuL] complex of $\mathbf{L}^3$.

In order to discuss the stability of the studied Cu(II) and Ni(II) complexes in comparison to complexes of other ligands, we propose to use the pM(II) value (Table 3), calculated at pH 7.4 for [L] = $10^{-5}$ M and [M(II)] = $10^{-6}$ M, which eliminates the differences in ligand protonation constants [27].

The pCu(II) values presented in Table 3 show that the methylphosphonate ligands $\mathbf{L}^1$, $\mathbf{L}^2$, $\mathbf{L}^4$ and $\mathbf{L}^5$ discussed in this paper have similar affinities for Cu(II) and all of them appear to be good complexing agents. Introduction of the 2-imidazole instead of 4(5)-imidazole moiety, $\mathbf{L}^1$–$\mathbf{L}^3$ [12], does not affect copper(II) binding. Nonetheless, this replacement has a dramatic influence on nickel binding. pNi(II) values of studied 2-imidazole ligands are few orders of magnitude greater than their 4(5)-imidazole analogs (Table 3) and therefore the ligands can be used as powerful chelating agents for Ni(II) ions which may compete with the low molecular weight bioligands such a histidine. Introduction of

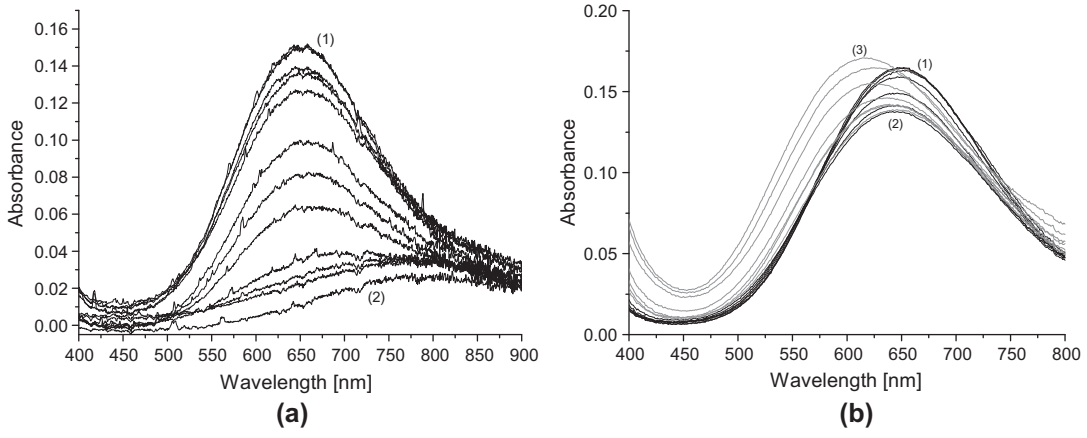


**Fig. 3.** (a) Absorption spectra collected during the acid titration of the 1:1 Cu(II)–$\mathbf{L}^3$ system; (1) pH 2.24, (2) pH 0.44; (b) absorption spectra collected during pH titration of the 1:2 Cu(II)–$\mathbf{L}^3$ system from pH 1.88 (1) through pH 5.20 (2) and up to pH 10.58 (3). I = 1 M ($NaClO_4$), $T$ = 25.0(2) °C; [Cu(II)] = $2 \times 10^{-3}$ M.

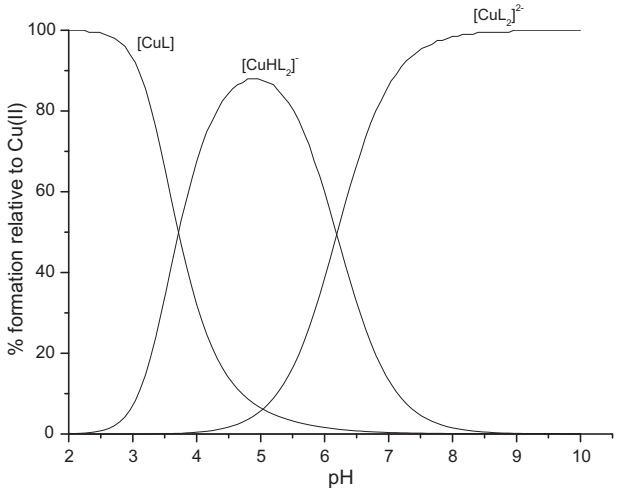


**Fig. 5.** Species distribution diagram for the Cu(II)–$\mathbf{L}^3$ system ([Cu(II)] = $2 \times 10^{-3}$ M, metal-to-ligand molar ratio 1:2).

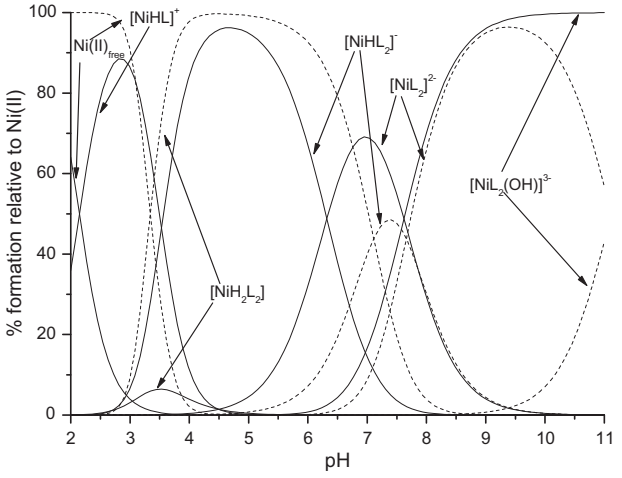


**Fig. 6.** Species distribution diagram for the Ni(II)–$\mathbf{L}^2$ system (solid line) and Ni(II)–$\mathbf{L}^3$ (dotted line). $\mathbf{L}^3$ – imidazole-4-methyl(N-benzylamino) phosphonic acid, [Ni(II)] = $2 \times 10^{-3}$ M, metal-to-ligand molar ratio 1:3.

**Table 3**
pM(II) values for various N-substituted imidazole (amino)methylphosphonates.[a]

| Ligand | pCu(II) | pNi(II) | Reference |
|---|---|---|---|
| $\mathbf{L}^1$ | 11.5 | 12.2 | This work |
| $\mathbf{L}^2$ | 13.5 | 13.0 | " |
| $\mathbf{L}^3$ | 21.9 | 28.7 | " |
| $\mathbf{L}^4$ | 11.5 | 16.9 | " |
| $\mathbf{L}^5$ | 13.8 | 14.0 | [12] |
| $\mathbf{L}^1$ | 12.8 | 7.4 | " |
| $\mathbf{L}^2$ | 12.9 | 8.6 | " |
| $\mathbf{L}^3$ | 12.5 | 8.4 | " |

[a] pM(II) = $-\log[M(II)]_{free}$ at pH 7.4 for [M(II)] = $10^{-6}$ M and [L] = $10^{-5}$ M. Abbreviations used: $\mathbf{L}^1$ – (amino)(1H-imidazol-4-yl)methyl phosphonic acid; $\mathbf{L}^2$ – imidazole-4-methyl(N-butyloamino) phosphonic acid; and $\mathbf{L}^3$ – imidazole-4-methyl(N-benzylamino) phosphonic acid.

*ortho*-pyridine as additional donor in the side chain significantly enhances the binding ability towards both, Cu(II) and Ni(II) ions (Table 3). The corresponding pCu(II) and pNi(II) values are increased by 8–16 orders of magnitude. The effectiveness of this compound may come from concomitant chelation of metal ions through the pyridine nitrogen donor together with imidazole and imino ones.

## 4. Conclusions

The obtained compounds (as ligands $\mathbf{L}^1$–$\mathbf{L}^5$) were evaluated for coordination of Cu(II) and Ni(II) ions. For all ligands, solution studies suggest formation of variously protonated mono- and bis-complexes, where copper and nickel coordination is realized through the nitrogen atoms of the imidazole and amino groups, supported by an oxygen from the phosphonate unit.

A series of new 2-imidazole ligands can be used as powerful chelating agents especially for Ni(II) ions. The presence of the 2-imidazole ring increases the binding ability of studied aminophosphonates when compared to the previously designed 4(5)-imidazole analogs. pNi(II) values of 2-imidazole ligands are few orders of magnitude greater than their 4(5)-imidazole derivatives. The present data clearly indicate the impact of imidazole moiety on the binding ability of aminophosphonate ligands.

Moreover, the introduction of *ortho*-pyridine as additional donor in the side chain significantly increases the binding ability towards both, Cu(II) and Ni(II) ions. The effectiveness of this compound may be due to concomitant chelation of metal ion through the imidazole, imino and pyridine nitrogen donors.

## Acknowledgments

The authors thank Professor Bogdan Boduszek (Wroclaw University of Technology) for $\mathbf{L}^1$ and $\mathbf{L}^2$ ligands used in this study and Professor Henryk Kozlowski (University of Wroclaw) for helpful discussions. This research was supported by the Polish Ministry of Science and Higher Education and Faculty of Chemistry, University of Wroclaw (105/10/E-344/M/2011) and by internal grant from the Faculty of Chemistry, Wroclaw University of Technology.

## References

[1] K. Popov, H. Ronkkomaki, L.H.J. Lajunen, Pure Appl. Chem. 73 (2001) 1641.
[2] V. Chavane, General Ann. Chim. 4 (1949) 352.
[3] R. Engel, Chem. Rev. 77 (1977) 349.
[4] T. Kiss, I. Lazar, in: V.P. Kukhar, H.R. Hudson (Eds.), Aminophosphonic and Aminophosphinic Acids Chemistry and Biological Activity, John Wiley and Sons Ltd., 2000, p. 285.
[5] J. Galezowska, E. Gumienna-Kontecka, Coord. Chem. Rev. (2011), doi:10.1016/j.ccr.2011.07.002.
[6] F. Orsini, G. Sello, M. Sisti, Curr. Med. Chem. 17 (2010) 264.
[7] L. Chruscinski, P. Mlynarz, K. Malinowska, J. Ochocki, B. Boduszek, H. Kozlowski, Inorg. Chim. Acta 303 (2000) 47.
[8] R. Lipinski, L. Chruscinski, P. Mlynarz, B. Boduszek, H. Kozlowski, Inorg. Chim. Acta 322 (2001) 157.
[9] J. Galezowska, P. Kafarski, H. Kozlowski, P. Mlynarz, V.M. Nurchi, T. Pivetta, Inorg. Chim. Acta 362 (2009) 707.
[10] W. Goldeman, M. Pyrkosz, E. Gumienna-Kontecka, B. Boduszek, Inorg. Chim. Acta 365 (2011) 391.
[11] B. Boduszek, Polish J. Chem. 75 (2001) 663.
[12] S. Sobek, B. Boduszek, H. Kozlowski, Inorg. Chim. Acta 355 (2003) 462.
[13] B. Boduszek, T.K. Olszewski, W. Goldeman, Experimental details and spectroscopic data will be given in an extensive paper devoted to various phosphorous derivatives of 2-imidazole, Tetrahedron, in preparation.
[14] P. Gans, B. O'Sullivan, Talanta 51 (2000) 33.
[15] P. Gans, A. Sabatini, A. Vacca, J. Chem. Soc., Dalton Trans. (1985) 1195.
[16] P. Gans, Data Fitting in the Chemical Sciences, John Wiley and Sons, Chichester, 1992.
[17] L. Alderighi, P. Gans, A. Ienco, D. Peters, A. Sabatini, A. Vacca, Coord. Chem. Rev. (1999) 311.
[18] H. Gampp, M. Maeder, C.J. Meyer, A.D. Zuberbühler, Talanta 32 (1985) 95.
[19] H. Gampp, M. Maeder, C.J. Meyer, A.D. Zuberbühler, Talanta 32 (1985) 257.
[20] H. Gampp, M. Maeder, C.J. Meyer, A.D. Zuberbühler, Talanta 33 (1986) 943.
[21] F.J.C. Rossotti, H.S. Rossotti, R.J. Whewell, J. Inorg. Nucl. Chem. 33 (1971) 2051.
[22] D.W. Marquardt, J. Soc. Ind. Appl. Math. 11 (1963) 431.
[23] M. Maeder, A.D. Zuberbühler, Anal. Chem. 62 (1990) 2220.
[24] B. Kurzak, A. Kamecka, K. Kurzak, J. Jezierska, P. Kafarski, Polyhedron 17 (1998) 4403.
[25] B. Kurzak, A. Kamecka, K. Kurzak, J. Jezierska, P. Kafarski, Polyhedron 19 (2000) 2083.
[26] R.J. Sundberg, R.B. Martin, Chem. Rev. 74 (1974) 471.
[27] W.R. Harris, C.J. Carrano, K.N. Raymond, J. Am. Chem. Soc. 101 (1979) 2213.